Validation of TRACE Code for Type-I Density Wave Oscillations in SIRIUS-N Facility, Which Simulates ESBWR

Masahiro Furuya, Yoshihisa Nishi and Nobuyuki Ueda Central Research Institute of Electric Power Industry (CRIEPI) 2-11-1 Iwado-kita, Komae, Tokyo 201-8511, JAPAN

Abstract

As a part of the international CAMP Program of the US Nuclear Regulatory Commission (USNRC), the best-estimate code TRACE is validated with the stability database of SIRIUS-N facility at high pressure. The TRACE code analyzed is version 5 patch level 2. The SIRIUS-N facility simulates thermal-hydraulics of the economic simplified BWR (ESBWR). The oscillation period correlates well with bubble transit time through the chimney region regardless of the system pressure, inlet subcooling and heat flux. Numerical results exhibits type-I density wave oscillation characteristics, since throttling at the core inlet shifts stability boundary toward the higher inlet subcooling, and throttling at the chimney exit enlarges unstable region and oscillation amplitude. Stability maps in reference to the inlet subcooling and heat flux obtained from the TRACE code agrees with those of the experimental data at 1 MPa. As the pressure increases from 2 MPa to 7.2 MPa, numerical results become much stable than the experimental results. This is because that TRACE underestimates two-phase frictional loss at such high pressure, since the natural circulation flow rate of numerical results is higher by up to 17 % than that of experimental results.

1 Introduction

Natural circulation is a key passive-safety driving force in nuclear reactors. In Economic Simplified Boiling Water Reactor (ESBWR, see Figure 1), the core is cooled by natural circulation flow. A chimney is installed on top of the core to enhance natural circulation flow rate. In order to investigate stability of ESBWR, we designed and constructed the SIRIUS-N facility. Figure 2 illustrates a schematic of SIRIUS-N facility, which is a scale copy of ESBWR. Experimental results with the SIRIUS-N facility indicates that ESBWR is susceptible to the flashing-induced density wave oscillations at low pressure [1] and type-I density wave oscillations at high pressure [2]. The acquired stability map suggests that ESBWR can start up with sufficient stability margin by pressurizing the reactor before withdrawing control rods [3].

In order to extend the stability database, numerical analysis is useful tool. There are two types of analysis: frequency domain and time domain codes. A frequency domain code is handy to predict stability boundary and decay ratio. For instance, the authors have conducted sensitivity study of liquid density variation [4], which cannot be varied in experiments. Although a time domain code is time-consuming, it accounts nonlinear terms and gives amplitude and waveform

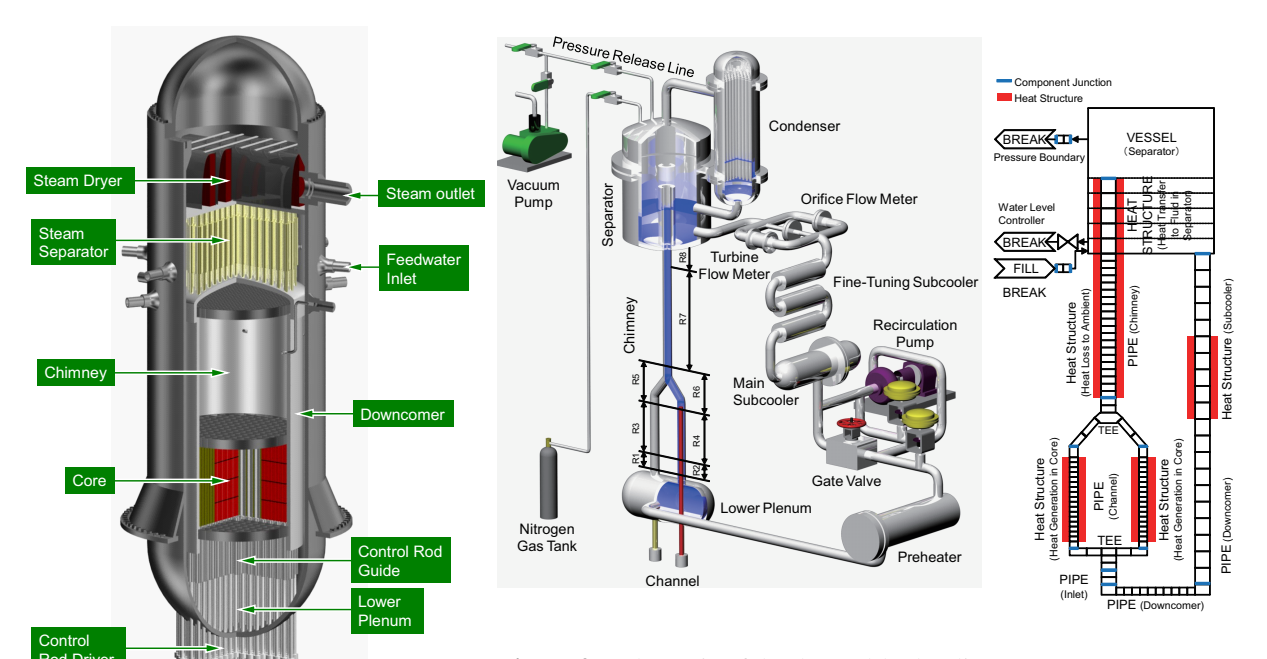


Figure 1: A cut-away of Natural Circulation BWR vessels (not to scale).

Figure 2: Schematic of the thermal-hydraulic loop of SIRIUS-N facility (not to scale). The Figure 3: Noding Di-SIRIUS-F is a full-height facility (13 m high) agram for the SIRIUSused to simulate boiling two-phase flow in the N Facility core of the ESBWR.

of limit-cycle oscillations. In the time-domain codes, TRACE code includes advanced bestestimate models to analyze transient of light water reactors. The TRACE code is developed US Nuclear Regulatory Commission (NRC) and distributed under the international CAMP-Program.

This paper addresses TRACE code validation against the SIRIUS-N stability database at high pressure ($P_s \ge 1$ MPa).

2 **Experimental Facility, SIRIUS-N**

The present code validation refers to the stability database with BWR regional stability facility SIRIUS-N*¹[3]. The SIRIUS-N facility equipped with artificial void-reactivity feedback on the basis of a set of acquired void fraction. This study refers to the pure thermal-hydraulic stability database without activating the artificial void-reactivity feedback.

The thermal-hydraulic loop of SIRIUS-N consists of two channels, a chimney, a separator, a condenser, a downcomer, a subcooler, and a preheater. A heater was inserted into each channel concentrically. The heated length, l_c , is 1.7 m and its profile is uniform. The chimney length, l_r , is 5.7 m.

In the figure 2, legends R0 through R8 indicate the measurement regions of differential pressure, and legend T indicates the measurement location of temperature. The thermocouples measuring fluid temperature are type K and 3.2 mm in diameter. Thermocouples measuring heater surface temperature were 0.5 mm in diameter, embedded and silver-brazed in the surface. A system pressure, P_s refers to the vapor pressure in the separator dome. An orifice is inserted into each

¹SIRIUS-N is abbreviation of SImulated Reactivity feedback Incorporated into thermal-hydraUlic Stability for Natural circulation BWR

Table 1: Comparison of the Facility with Natural Circulation BWR

System Pressure, P_s	0.1MPa		7.2MPa	
Target	Reactor	Facility	Reactor	Facility
Flashing Parameter, N_f	67	46	0.057	0.036
Froude Number, Fr	10.5.10-4	$7.6 \cdot 10^{-4}$	0.058	0.053
Phase Change Number, N_{pch}	11.6	13.1	3.7	3.7
Subcool Number, N_{sub}	9.0	9.0	0.58	0.58
Nondimensional Drift Velocity, v_{gj}	1.32	1.97	0.138	0.183
Ratio of Vapor Density to Liquid, R_{gl}	6.2·10-4	6.2·10-4	0.052	0.052
Ratio of Vapor Density at the Channel Inlet to Chimney Exit, ρ_{gg}/ρ_{gl}	2.01	1.63	1.01	1.01
Friction Coefficient in the Channel, ξ	6.9	5.7	3.4	2.7
Orifice Coefficient at the Channel Inlet, $\zeta_{c,in}$	10~50	30	10~50	30
Orifice Coefficient. at the Chimney Exit, $\zeta_{r,ex}$	20~40	21	20~40	21
Nondimensional				
Downcommer Cross Sectional Area, $A_{d,e}$	1.05	1.11	1.05	1.11
Nondimensional Chimney Cross Sectional Area, A_r	2.59	2.47	2.59	2.47
Nondimensional Chimney Length, L_r	3.34	3.38	3.34	3.38

Table 2: Number of Mesh in Sensitivity Study

	Coarse	Medium	Fine
Component	Mesh	Mesh	Mesh
Channel	19	40	40
Channel Heater	17	34	34
Chimney	25	50	100
Vertical Downcomer	20	50	100
Horizontal Downcomer	12	12	12

channel inlet. Its local pressure loss coefficient κ_i is 19. Comparison of SIRIUS-N facility to the representative natural circulation BWR is summarized in table 1 [3].

3 Numerical Analysis

Thermal-hydraulic stability was investigated with TRACE version 5.0 patch level 2, developed by United States Nuclear Regulatory Commission (USNRC). Figure 3 shows a noding diagram, which describes a flow network of SIRIUS-N facility. A VESSEL component represents the separator in SIRIUS-N facility. The uppermost cell in the VESSEL component is connected to a BREAK component to maintain the system pressure the same as the experiment. Nearly saturated water ($\Delta T_{sub} = 4$ K) flows into the lowermost cell in the component. Another BREAK component is attached to the same cell through a valve. The valve controls the void fraction to maintain the water level the same as the experiment.

The water in the separator flows into vertical downcomer, and then horizontal downcomer, which are modeled with PIPE components. A heat structure is attached in the middle of the downcomer to cool down the water to set the constant subcooling at the channel inlet. In the TEE component, the water flow divided into two to travel through two channels. Other heat structures are attached in the channels to apply heat to the flow as the simulated reactor core. These channels are modeled with PIPE components instead of CHAN component, because of the simplicity. The outflow from two channel merges in a TEE component to path through the chimney section. The flow discharges above the water level in the separator. The heat structure attached to the lower and upper PIPE components calculates heat loss to the environment and

separator, respectively. The heat loss to the ambient is substantially small, since the surrounding heat insulation is rock wool.

4 Results and Discussions

4.1 Verification

Consistency of the input model is verified with SNAP version 2.0 [5]. A parametric study was conducted to verify the temporal and spatial noding. The spatial mesh size must be adequately small to capture a spatial variation of the void propagation. The size should not, in turn, be too small to induce numerical instability.

Table 2 summarizes the number of spatial meshes in the present noding. In order to capture the void propagation in the chimney, which dominates instability, three different numbers of mesh in the chimney were investigated parametrically: 25 for coarse case, 50 for intermediate case, and 100 for fine case.

Figure 4 shows sensitivity study for the spatial mesh size. The figure 4(a) shows time-average values of liquid velocity at channel inlet. The values are averaged for every one degree Kelvin and plotted as the different line styles. Experimental data are plotted as different symbols classified by the stability: 'O' is stable and 'D' is unstable. In the experimental campaign, the flow is classified as unstable when the standard deviation of velocity at the channel inlet exceeds 10 percent than the time-average value. All three mesh-size cases coincide with each other. The TRACE results underestimate experimental data at lower subcooling, since the two-phase friction factor may be estimated lower.

The figure 4(b) shows instantaneous values and standard deviation of the velocity. Even when the maximum standard deviation exceeds 20 %, the instantaneous values oscillate around the time-average values as shown in the figure 4(a). In addition, waveforms were sinusoidal for both experimental and numerical results. The observed oscillations are therefore, dynamic instability. Although the standard deviation enlarges with increasing the number of mesh, the difference is small. In the rest of calculation, we use the coarse mesh, since it gives the same results within the smallest calculation time.

Figure 5 shows temporal sensitivity. The TRACE code requires a maximum allowable time step. We set 50 ms for the base case. In the sensitivity study, we compare results of 50 ms to 5 ms. The maximum allowable time step are adopted as the time step except the initial calculation phase. Both time-average values in the figure 5(a) and instantaneous values in figure 5(b) indicate that one-tenth time step does not affect the stability results. The maximum allowable time step is fixed in this study due to calculation efficiency.

4.2 Waveform

Figure 6 shows a representative time trace of channel inlet velocity acquired when $P_s = 2$ MPa and q'' = 304 kW/m². Figure 6 (a)-(c) were acquired for different inlet subcooling in the vicinity of the stability boundary at lower subcooling. Figure 6 (a) ($\Delta T_{sub} = 25.3$ K) shows both sinusoidal waveforms. Both amplitude and period of oscillations coincide with each other. The period of oscillations in TRACE is slightly shorter than that in the experiment. Figure 6 (b)

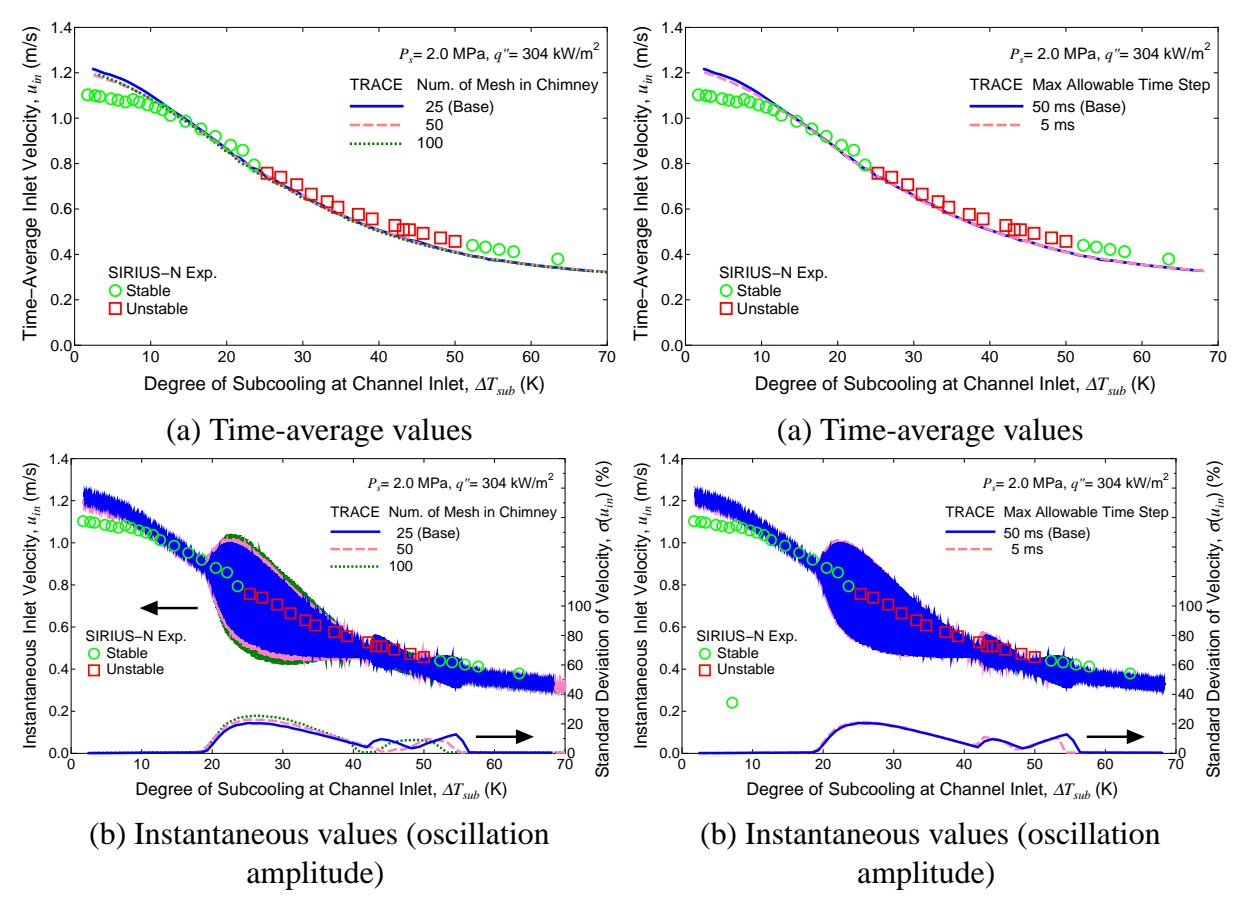


Figure 4: Sensitivity of Spatial Mesh Size

Figure 5: Effect of Maximum Allowable Time Step

 $(\Delta T_{sub} = 22.1 \text{ K})$ shows stable waveform in the experiment, while still unstable waveform with almost the same amplitude as Figure (a). Figure 6 (c) $(\Delta T_{sub} = 18.5 \text{ K})$ shows both stable waveforms. These waveforms indicates TRACE predicts the stability boundary at lower subcooling lower.

4.3 Stability Map

Figure 7(a) shows a stability map at 1 MPa in reference to the inlet subcooling and heat flux. The internal region of thick red-curve indicates unstable region determined by SIRIUS-N experiment [2]. In the experiment, instability was observed during a certain subcooling range. There is no instability observed below 90 kW/m². The results from TRACE is plotted as a bubble plot manner, where a symbol size is standard deviation of the inlet velocity. Example symbol sizes (1, 10 and 20 %) are plotted as legends in the figure 7. In the experiments when $P_s \ge 1$ MPa, the flow is classified as unstable when the standard deviation exceed 10 %. The subcooling range where instability occurs in TRACE agrees with that in SIRIUS-N experiment. Instability were observed in the TRACE results below 90 kW/m². Instability is commonly observed in the low heat flux range in the time-domain code such as TRACE and TRAC-G codes [6], and in the frequency domain codes. The amplitude of oscillation in experiments are significantly small, and the flow is therefore, classified in stable.

Figure 7(b) shows a stability map at 2 MPa. Instability occurs during a certain subcooling in the TRACE results, though the range shifts to the lower subcooling to that of experimental results. Although the range decrease with decreasing heat flux, instability occurs below the limit of experimental range.

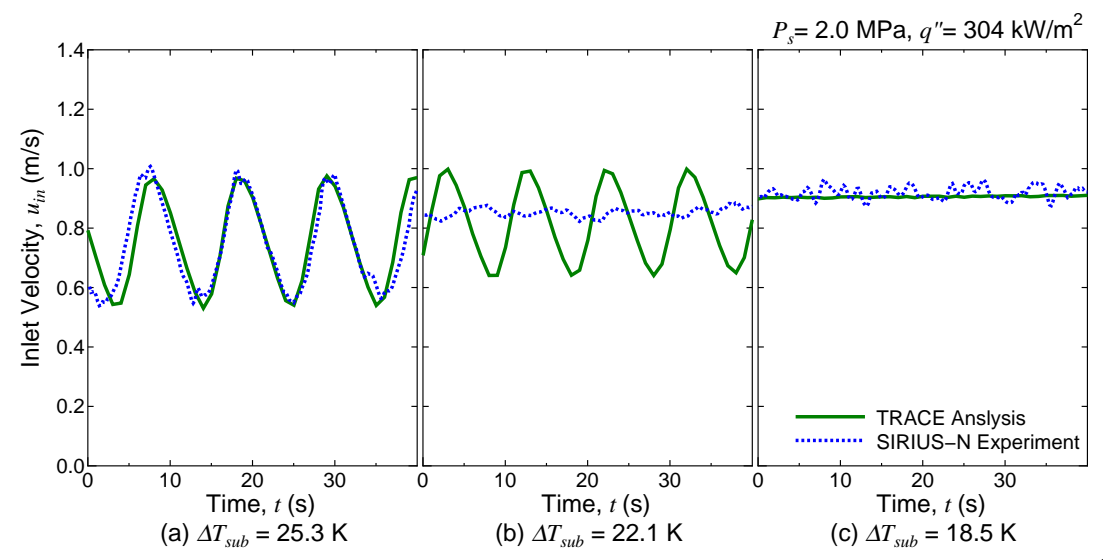


Figure 6: Representative Time Trace of Inlet Velocity Acquired When $P_s = 2$ MPa and q'' = 304 kW/m²

Figure 7(c) shows a stability map at 4 MPa. The standard deviations at 4 MPa becomes much smaller than those at 1 MPa and 2 MPa. The instability observed in the TRACE results is involved in the SIRIUS-N stability boundary.

Figure 7(d) shows a stability map at 7.2 MPa. All the points calculated are stable even where the instability occurred in SIRIUS-N experiments.

4.4 Instability Mechanism

An oscillation period infer the dominant response time of instability [7]. The experimental campaign of SIRIUS-N reveals that the oscillation time correlates well with transit time of single-phase liquid at relatively low pressure (0.1 - 0.5 MPa) [1] and that of bubbles at relatively high pressure (1 - 7.2 MPa) [2] in the chimney. This is because the dominant phenomena are transit of hot liquid in the chimney to flash at relatively low pressure, and transit of bubbles in the chimney to gain driving force of natural circulation at relatively high pressure.

Figure 8 shows relationship of oscillation time to transit time of bubbles. The transit time of bubbles is calculated as a chimney length divided by the vapor-phase velocity. The vapor-phase velocity for the experiment is estimated on the basis of drift-flux model. Note that there is no unstable data available for the TRACE data at 7.2 MPa. The oscillation period from TRACE results correlates well with the transit time of bubbles in the chimney regardless of the system pressure, inlet subcooling, and heat flux. A ratio of transit time to the oscillation time, $\tau_{fo}/\tau_{pr,g}$ ranges 1.1 to 1.8 in the experiments. The TRACE results falls roughly in the same range. The fact explores that the TRACE demonstrates representative type-I density wave oscillations [8].

Figure 9 shows an effect of friction factor when $P_s = 2$ MPa and q'' = 304 kW/m². In addition to the base case, three cases are investigated: doubled local pressure-loss coefficient at the channel inlet, doubled local pressure-loss coefficient at the chimney exit, and tenfold surface-roughness for all the components. In the base case, surface roughness is set as 6 μ m. According to the figure 9(a) the time-average inlet velocity decreases up to 9 % decrease at lower subcooling, since these modifications increase pressure loss.

Figure 9(b) shows standard deviation in terms of inlet subcooling. In forced circulation system, inlet throttling stabilizes the flow. In natural circulation system, it shifts unstable region toward

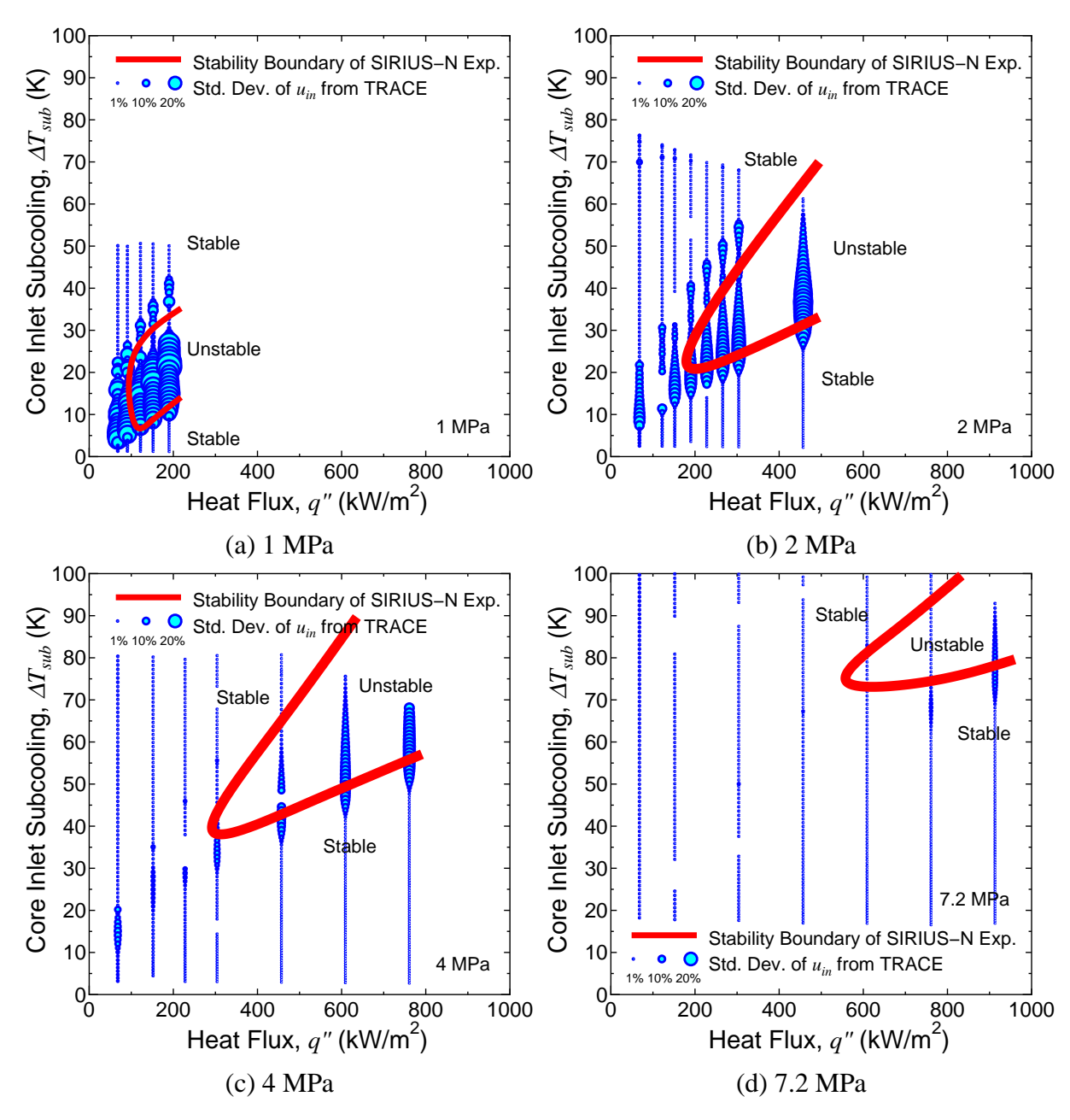


Figure 7: Stability Maps: Bubble Plot in Reference to Standard Deviation of Inlet Velocity

the higher subcooling [9]. According to the figure, the doubled inlet restriction shifts unstable region to the higher subcooling by 8 K.

The doubled exit-restriction destabilized the flow, thereby enlarging the unstable region and amplitude of oscillations. The tenfold surface roughness increases pressure loss slightly in both single-phase and two-phase regions. It shifts unstable region toward higher subcooling by 2 K. Those TRACE results are representative characteristics of Type-I density wave oscillations.

4.5 Solution Scheme

In TRACE code, a set of equations are solved by SETS (stability-enhancing two-step) solution scheme. Since SETS numerics allows the material Courant limit to be exceeded, one can use a large time step for slow transients. One may wonder if SETS dampen physical limit cycle oscil-

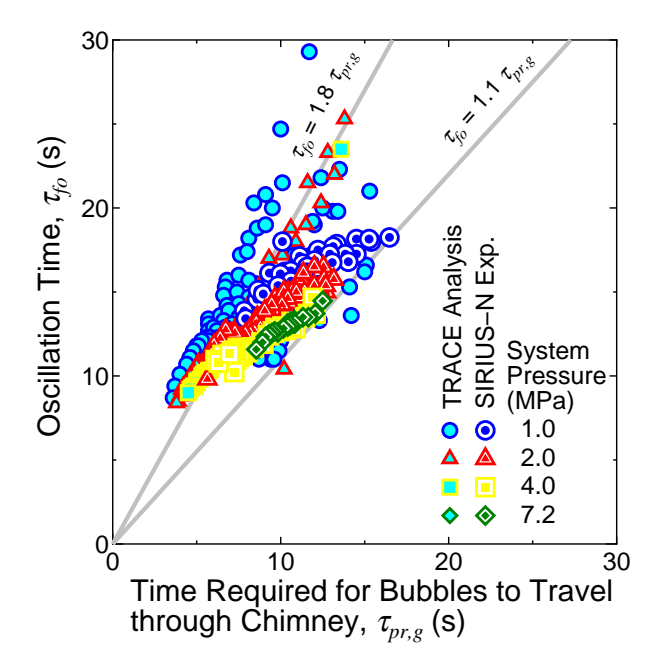


Figure 8: Relationship of Oscillation Period to Transit Time

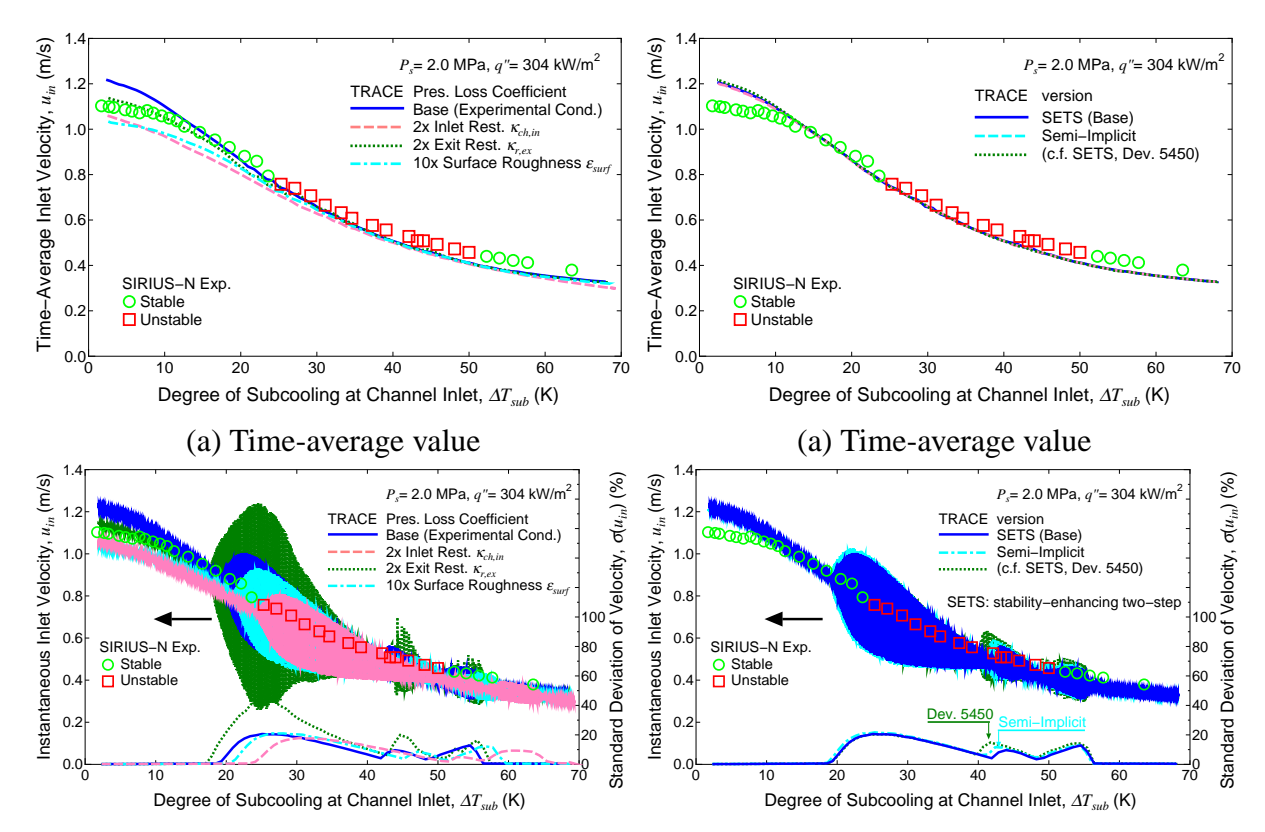
lations significantly. As an alternative solution scheme, semi-implicit scheme is implemented in TRACE version 5.0.

Figure 10 shows comparison of solution scheme when $P_s = 2$ MPa and q'' = 304 kW/m². Figure 10 (a) shows the time-average value. There are negligibly small deviations among three lines: SETS scheme (version 5.0 patch level 2 and development version 5.450), semi-implicit (version 5.0 patch level 2). Figure 10 (a) shows the instantaneous value. Semi-implicit scheme gives slightly larger amplitude along the entire subcooling range. The development version 5.450 gives larger amplitude than other two schemes where $40 \le \Delta T_{sub} \le 55$, while it gives the same amplitude elsewhere. The stability boundary does not differ among three solution schemes.

5 Concluding Remarks

TRACE code analysis was performed to validate the stability experiments with SIRIUS-N facility. The following conclusions are drawn:

- (1) The maximum allowable time step and spatial mesh are insensitive on the stability within the ranges of investigation.
- (2) Stability map of TRACE at 1 MPa agrees with that of SIRIUS-N facility qualitatively, though instability observed in the low heat flux range below the stability limit of experiment. Increasing pressure shrinks unstable region toward the lower subcooling of unstable range in the experiments. Instability is not observed at 7.2 MPa, even where instability was observed in the experiments. This is because TRACE underestimates two-phase frictional loss, as TRACE predicts inlet velocity by up to 17 % higher than that of experiments.
- (3) The TRACE code demonstrates Type-I density wave oscillation characteristics: The oscillation period correlates well with the transit time of bubbles in the chimney regardless



(b) Instantaneous value (oscillation amplitude) (b) Instantaneous value (oscillation amplitude)

Figure 9: Effect of Frictional Pressure Loss Coefficients

Figure 10: Effect of Solution Scheme

of the system pressure, inlet subcooling, and heat flux. Inlet throttling shifts unstable region toward the higher subcooling. Exit throttling enlarges unstable region and amplitude of oscillations.

(4) Semi-implicit scheme gives slightly larger amplitude than SETS scheme along the entire subcooling range. The development version 5.450 gives larger amplitude than version 5.0 patch level 2 at relatively higher subcooling. The stability boundary does not differ among these three solution schemes.

ACKNOWLEDGEMENTS

The authors are grateful for Dr. James T. Han of USNRC, who promote the cooperative tasks of the code validation. They would also like to express our appreciation toward Dr. Wayne Marquino of GE Hitachi Nuclear Energy, who allow them to refer EBSWR design parameters in the present task.

REFERENCES

[1] M. Furuya, F. Inada, T. H. J. J. Van der Hagen, "Flashing-Induced Density Wave Oscillations in a Natural Circulation Loop with a Chimney - Mechanism of Instability and Stability Map -", Nuclear Engineering Design 235 (15) (2004) 1557–1569.

- [2] M. Furuya, F. Inada, T. H. J. J. Van der Hagen, "Characteristics of Density Wave Oscillations in a Natural Circulation BWR at relatively High Pressure", J. Nucl. Sci. Technol. 42 (2) (2004) 191–200.
- [3] M. Furuya, "Experimental and Analytical Modeling of Natural Circulation and Forced Circulation BWRs Thermal-Hydraulic, Core-Wide, and Regional Stability Phenomena", Ph.D. thesis, Faculty of Applied Science, Delft Univ. Tech., the Netherlands, ISBN 1-58603-605-X (2006).
- [4] M. Furuya, D. D. B. Van Bragt, T. H. J. J. Van der Hagen, W. J. M. De Kruijf, "Effect of Liquid Density Difference on Two-Phase Flow Instability", Proc. 9th Int. Meeting on Nucl. Reactor Thermal-Hydraulics F-2 (1999) (CD–ROM Publication).
- [5] USNRC, TRACE version 5 patach level 2 Code Manuals (2010).
- [6] Y. K. Cheung, L. A. Klebanov, M. Furuya, "TRACG Analyses of Two-Phase Flow Instability Data from SIRIUS Loop at Relatively High System Pressure", Proceedings of 9th International Conference on Nuclear Engneering (ICONE-9) ICONE-9185, Nice, France.
- [7] J. A. Bouré, A. E. Bergles, L. Tong, "Review of Two-phase Flow Instability", Nucl. Engng. Des. 25 (1973) 165–192.
- [8] K. Fukuda, T. Kobori, "Classification of Two-Phase Instability by Density Wave Oscillation Model", J. Nucl. Sci. Technol. 16 (1979) 95.
- [9] M. Furuya, F. Inada, A. Yasuo, "Inlet Throttling Effect on the Boiling Two-Phase Flow Stability in a Natural Circulation Loop with a Chimney" 37 (2001) 111–115.